Journal of Medicinal and Chemical Sciences 7 (2024) 689-702

Journal of Medicinal and Chemical Sciences

Journal homepage: http://www.jmchemsci.com/

Original Article

Advancements in Fe_3O_4/PANI Nanocomposite Film Technology: Synthesis and Characterization

Yenni Darvina[1], Desnita Desnita [1*], Rahadian Zainul[2], Imtiaz Ali Laghari[3], Azril Azril[4], Mohammad Abdullah[5]

[1]*Department of Physics, Faculty of Mathematics and Natural Sciences, Universitas Negeri Padang, Indonesia*
[2]*Department of Chemistry, Faculty of Mathematics and Natural Sciences, Universitas Negeri Padang, Indonesia*
[3]*Department of Electrical Engineering, Quaid-e-Awam University of Engineering, Science and Technology, Campus Larkana, Sindh, 67480, Pakistan*
[4]*Department of Biomedical Engineering, National Cheng Kung University, Tainan City, Taiwan*
[5]*Chemical Engineering Studies, College of Engineering, University Teknologi MARA Johor Branch, Pasir Gudang Campus, Bandar Seri Alam, 81750 Masai, Pasir Gudang, Johor Bahru, Johor, Malaysia*

ARTICLEINFO

Article history

Receive: 2024-12-15
Received in revised: 2024-02-09
Accepted: 2024-02-13
Manuscript ID: JMCS-2401-2439
Checked for Plagiarism: **Yes**
Language Editor Checked: **Yes**

DOI:10.26655/JMCHEMSCI.2024.5.5

KEYWORDS

Fe_3O_4/PANI Nanocomposites
Magnetic Nanomaterials
Sol-Gel Process
Spin Coating Method
Structural and Electrical Characterization

ABSTRACT

In this study, the synthesis of Fe_3O_4 /PANI nanocomposites is achieved by employing a spin coating technique, which involves the initial preparation of Fe_2O_3 from iron sand through magnetic separation and ball milling. The Fe_3O_4 precursor is then combined with polyaniline (PANI) at different concentrations (30%, 40%, 50%, 60%, and 70%) using a sol-gel process. The resulting Fe_3O_4 /PANI gel mixture is spin-coated onto glass substrates and dried. The nanocomposite films undergo extensive characterization through X-ray Diffraction (XRD), Scanning Electron Microscopy (SEM), Vibration Sample Magnetometry (VSM), and electrical measurements using an LCR meter. Our findings show a correlation between Fe_3O_4 concentrations and crystal size, observed as a decrease from 30% to 40%, an increase at 50%, and a subsequent decrease from 60% to 70%. Fourier-transform infrared spectroscopy (FTIR) confirms the chemical bonding between Fe_3O_4 Fe_2O_3 and PANI. SEM images reveal the layer thickness varies with concentration, measured as 5.02 µm, 16.54 µm, 17.82 µm, 19.36 µm, and 24.4 µm, respectively. Electrical properties indicate resistance values of 7.36 mΩ, 8.388 mΩ, 8.101 mΩ, 8.53 mΩ, and 3.53 mΩ for the respective Fe_3O_4 concentrations, with corresponding capacitance values. This study elucidates the structural and electrical properties of Fe_3O_4 /PANI nanocomposites, highlighting their potential for diverse applications.

* Corresponding author: Desnita
✉ E-mail: desnita343@gmail.com

GRAPHICAL ABSTRACT

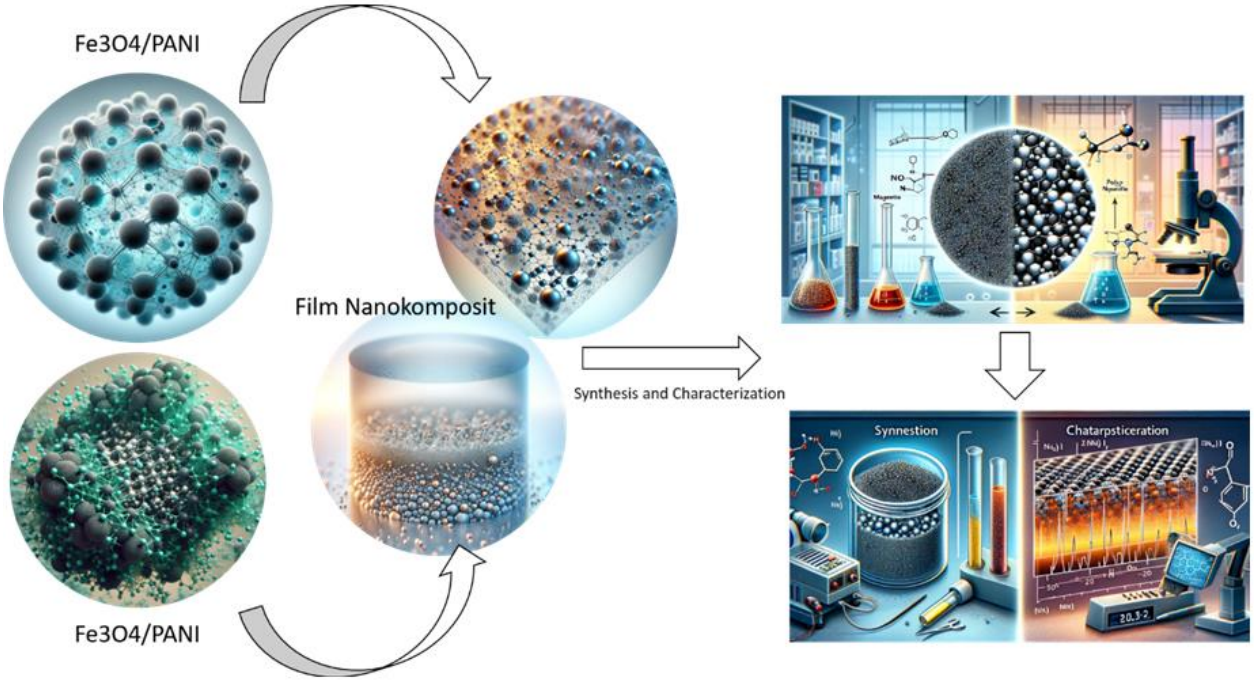

Introduction

The integration of electronic devices into daily life has escalated energy demands, underscoring the critical need for sustainable energy sources and advancements in energy storage technologies. Among various solutions, lithium batteries stand out for their pivotal role in powering electronics, benefiting from attributes like high energy density and the absence of a memory effect, facilitating their widespread adoption [1-9]. Despite their advantages, lithium batteries grapple with significant safety, economic, and environmental concerns, necessitating the exploration of safer and more sustainable alternatives [10-17]. Addressing the limitations of conventional lithium battery materials, such as graphite, which suffers from electrochemical constraints that impede lithium ion mobility and diminish energy efficiency, research has shifted towards innovative materials. Fe_3O_4 magnetite nanoparticles have gained prominence as a superior alternative due to their high theoretical capacity (1000 mAh/g), abundance, and cost-effectiveness, offering a potential breakthrough in electrode material technology [18-25]. The employment of nanostructured materials is a strategic response to these challenges, aiming to enhance electrochemical performance by optimizing ion and electron transport pathways and expanding electrode contact surfaces, thus facilitating improved charge/discharge kinetics and elevated energy capacities [26-31]. Parallelly, the field of supercapacitors is witnessing significant interest owing to their remarkable specific capacitance, robustness, high power output, and eco-friendly characteristics. These features render supercapacitors ideal for applications in portable electronics and electric vehicles, demanding advancements in electrode materials to overcome the limitations posed by conventional options like activated carbon and transition metal oxides [32-54]. The quest for materials that blend high conductivity with structural advantages has led to the exploration of innovative composites. This manuscript presents a study focused on the development of a supercapacitor electrode material comprising a nanocomposite of Fe_3O_4 metal oxide and PANI conductive polymer.

This study aims to leverage the unique properties of supercapacitors and address the current gaps in energy storage solutions by enhancing the performance of supercapacitors through the introduction of Fe_3O_4 @conductive polymer nanocomposites. This approach is particularly innovative as it utilizes Fe_3O_4 synthesized from iron sands sourced from West Sumatra, offering a novel pathway to sustainable and efficient energy storage [61-62].

By targeting the advancement of electrode materials for both lithium batteries and supercapacitors, this study endeavours to contribute significantly to the field of energy storage, addressing both the challenges of current technologies and the pressing demand for sustainable energy solutions.

Materials and Methods

Iron sand from West Sumatra, Indonesia, was used to synthesize Fe_3O_4 nanoparticles. Analytical-grade reagents: $FeCl_2{\cdot}6H_2O$, ammonium persulfate, HCl, and aniline monomer (C_6H_5N, 99%), were obtained from Sigma Aldrich and used as received.

Synthesis of Fe_3O_4 nanoparticles

The process started with the magnetic separation of iron sand to isolate magnetite-rich fractions, followed by cleaning and drying. The material underwent further magnetic separations and was then processed in a high-energy milling machine, with a ball-to-sample weight ratio of 10:1, for 30 hours to achieve a uniform Fe_3O_4 phase.

Synthesis of PANI/ Fe_3O_4 nanocomposite

Fe_3O_4 nanoparticles were mixed with hydrochloric acid (35% by volume) to prepare the precursor. $FeCl_2{\cdot}6H_2O$ was reacted with the nanoparticles in hydrochloric acid, using 2 mL of HCl per gram of magnetite. The nanocomposite was synthesized via *in situ* polymerization, varying Fe_3O_4 concentrations from 30% to 70%. Ammonium persulfate was added gradually over four hours. The product was then washed, dried, and prepared for spin coating to form thin layers, which were dried at 60 °C.

Characterization of PANI/ Fe_3O_4 nanocomposite

The Fe_3O_4 /PANI samples underwent characterization using X-ray diffraction (XRD), scanning electron microscopy (SEM), and electrical testing with an LCR meter to evaluate their crystal structure, morphology, and electrical properties.

Results and Discussion

Structure of Fe_3O_4/PANI nanocomposite

The structural characteristics of Fe_3O_4 /PANI nanocomposites with varied Fe_3O_4 concentrations were elucidated through X-ray diffraction (XRD) analysis. Figure 1 presents the diffraction patterns for the nanocomposites at Fe_3O_4 concentrations of 30%, 40%, 50%, 60%, and 70%. XRD results show variations in peak intensities and widths, reflecting differences in crystal sizes. The peaks are assigned to PANI (Powder Diffraction File code: 00-060-1168) and Fe_3O_4 (Powder Diffraction File code: 01-078-3149).

Incorporating the analysis from recent studies, we can enhance the understanding of the relationship between Full Width at Half Maximum (FWHM) values and crystal sizes, particularly through the lens of Scanning Electron Microscopy (SEM) images. The FWHM values, as indicators of crystal perfection and size in X-ray diffraction patterns, offer a quantitative measure of crystal dimensions. A direct correlation between FWHM values and crystal sizes has been observed, where smaller FWHM values often signify larger crystalline structures due to reduced strain and defects within the crystal lattice. This relationship is critical in materials science, especially for optimizing the properties of nanocomposites and thin films where crystal size plays a pivotal role in determining the material's electrical, optical, and mechanical properties. Studies have demonstrated that the addition of certain elements, such as Zn in CdS films, can significantly alter the structural and optical properties of the resulting compounds, affecting their bandgap and, consequently, their application potential in devices like solar cells.

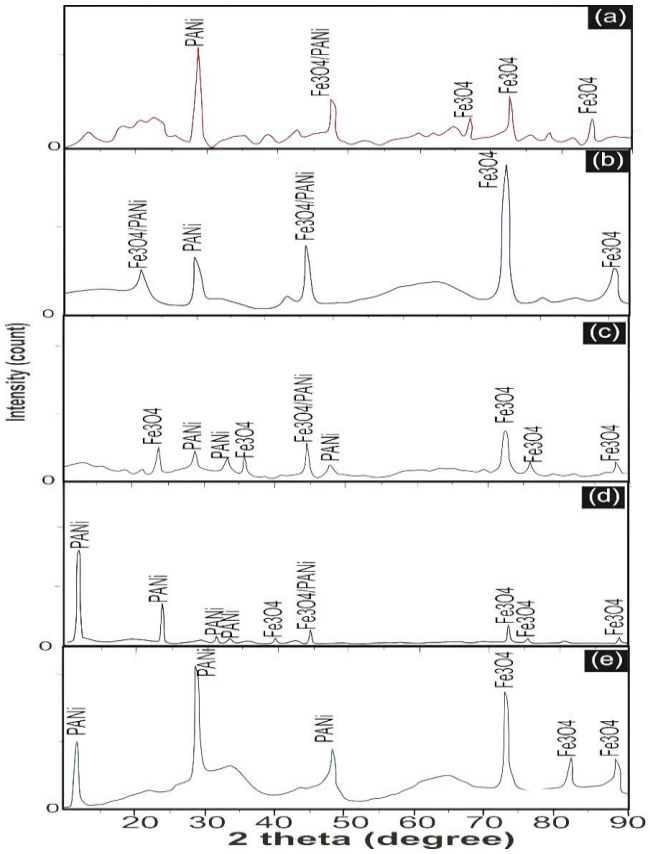

Figure 1: Diffraction patterns of Fe_3O_4 /PANI nanocomposite at various Fe_3O_4 concentrations: (a) 30%, (b) 40%, (c) 50%, (d) 60%, and (e) 70%

The alteration in crystal size and structure, as influenced by composition and processing conditions, can be meticulously analysed through SEM imaging, providing a visual and quantitative assessment of these changes [63-65]. SEM images not only complement the data obtained from FWHM measurements by offering a direct visual representation of the crystal sizes and shapes, but also help in understanding the morphological evolution of the material as a function of different synthesis conditions or compositional variations. This dual approach of combining XRD analysis with SEM imaging forms a comprehensive methodology for investigating and tailoring material properties at the nanoscale. Analysis reveals that crystal size is smaller at a 40% concentration compared to 30%, 60%, and 70% concentrations, with the largest crystal size at 50% concentration. Subsequently, crystal size diminishes at 60% and 70% concentrations. In addition, Full Width at Half Maximum (FWHM) values correlate directly with crystal sizes, where smaller FWHM values indicate larger crystals. FWHM values increase from 30% to 70% concentration, signifying a reduction in crystal size.

SEM imaging was utilized to examine the cross-sectional thickness of Fe_3O_4 /PANI nanocomposite layers. Figure 2 displays cross-sectional images for 30%, 40%, 50%, 60%, and 70% concentrations. The thickness increases with concentration, revealing a direct relationship between Fe_3O_4 concentration and nanocomposite layer thickness. Specifically, layer thicknesses are 5.02 µm, 16.54 µm, 17.82 µm, 19.36 µm, and 24.4 µm for 30%, 40%, 50%, 60%, and 70% concentrations, respectively. This trend underscores that higher Fe_3O_4 concentrations lead to denser layers, attributable to more Fe_3O_4 particles integrating into the polymer matrix [66-68]. The integration of SEM imaging in the analysis further solidifies the understanding of how changes in concentration affect the structural attributes of nanocomposites, directly correlating with FWHM findings and providing a more comprehensive picture of material behaviour across different concentrations.

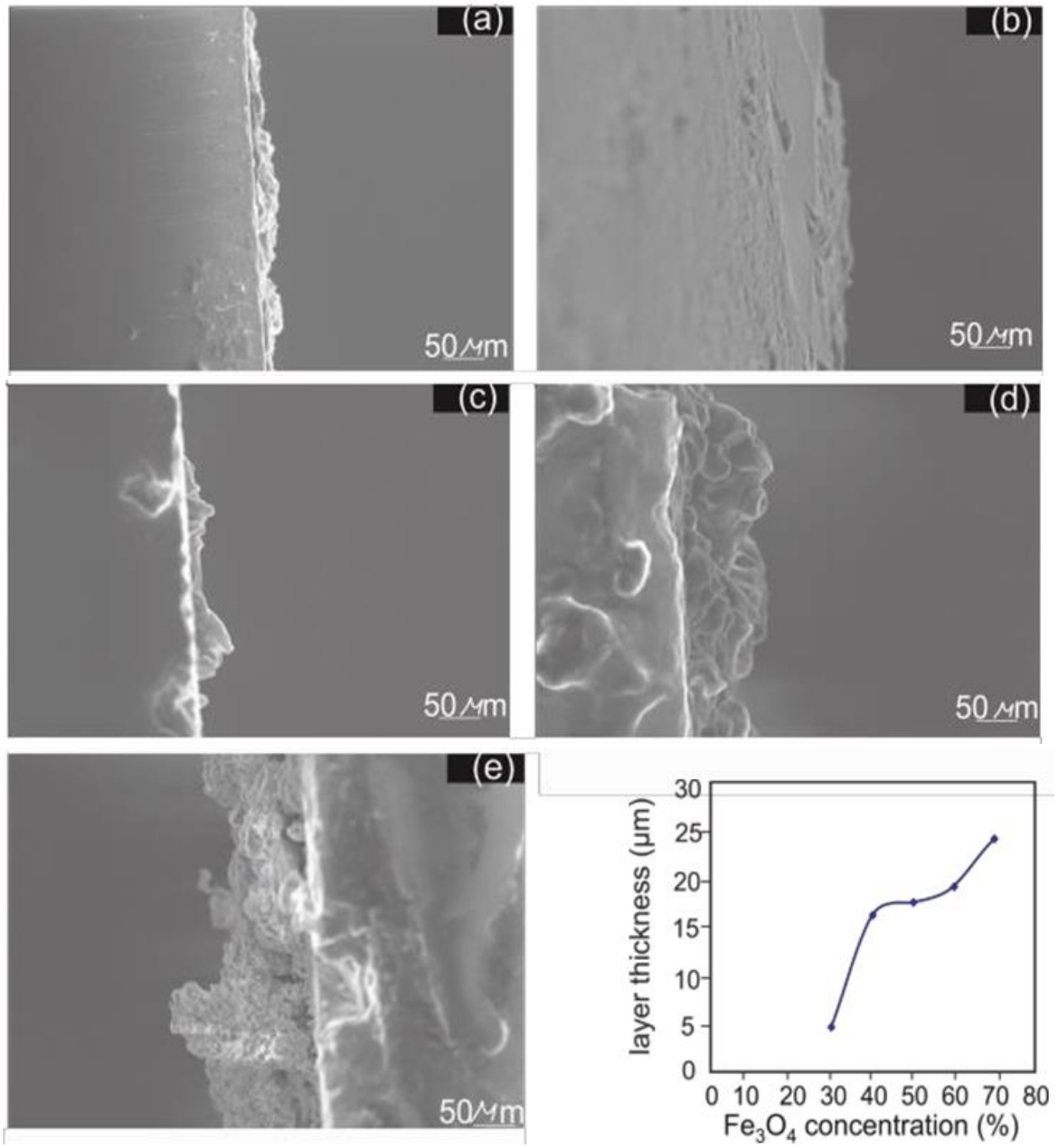

Figure 2: Cross-sectional images of Fe_3O_4 / PANI nanocomposite layers at varying Fe_3O_4 concentrations. Insets show the relationship between Fe_3O_4 concentration and layer thickness

Upon examining the SEM images in Figure 2, which showcase cross-sectional views of Fe_2O_3/PANI nanocomposite layers at different Fe_3O_4 concentrations, a clear trend is evident in the morphology and layer thickness as the concentration of Fe_3O_4 increases. The images labelled (a) through (e) correspond to increasing concentrations of Fe_3O_4 from 30% to 70%. Image (a) shows a relatively smooth and uniform layer, indicative of a lower concentration composite. As the concentration rises, images (b) and (c) display progressively rougher textures and increased irregularity, suggesting a densification of the nanocomposite structure with more Fe_3O_4 particles becoming embedded within the polymer matrix. Further increases in Fe_3O_4 concentration are reflected in images (d) and (e), where the layers not only become thicker, but also exhibit a more pronounced ruggedness and porosity. This is consistent with the inset graph, which plots layer thickness against Fe_3O_4 concentration, demonstrating a nonlinear increase in thickness. The thickest layer at the 70% concentration shows significant morphological changes, including larger, more distinct particles and a more complex surface topology compared to the

smoother layers at lower concentrations. These observations support the idea that the Fe_3O_4 concentration within the nanocomposite has a significant impact on both the microstructural and macrostructural scales. The microstructural scale, indicated by the surface topology and particle size visible in the SEM images, suggests that higher Fe_3O_4 concentrations lead to greater agglomeration and potentially affect the electrical and mechanical properties of the nanocomposite. On the macrostructural scale, the overall increase in layer thickness could impact the feasibility of layer application and the performance of the nanocomposite in practical devices. The morphological features observed in these SEM images are crucial for understanding the material's performance characteristics. The rugged and porous structure observed at higher Fe_3O_4 concentrations could potentially enhance the surface area of the electrode, which is beneficial for applications like supercapacitors that rely on surface reactions. Conversely, the increased roughness and irregularity at higher concentrations might lead to mechanical instability, which would be a trade-off against the enhanced electrical properties. Therefore, optimizing the Fe_3O_4 concentration in the Fe_3O_4/PANI nanocomposite is essential for balancing these properties to meet specific application requirements. Overall, the SEM analysis provided in Figure 2 affords a comprehensive understanding of the material's structural evolution with changing Fe_3O_4 concentration, offering insights into the trade-offs and considerations necessary for the application-specific optimization of Fe_3O_4 /PANI nanocomposites.

The study demonstrates that Fe_2O_3 concentration not only affects crystal size, but also significantly impacts the thickness of the nanocomposite layers, highlighting the direct correlation between material composition and structural properties.

Electrical properties of Fe_3O_4/PANI nanocomposite

The study of the electrical properties of Fe_3O_4/PANI nanocomposite layers is crucial to this research. Electrical resistance and capacitance were precisely measured using an LCR meter. Figure 3 demonstrates the correlation between Fe_3O_4 concentration in the nanocomposites and their electrical resistance.

XRD results show a clear trend in resistance values at Fe_3O_4 concentrations of 30%, 40%, 50%, 60%, and 70%, recorded as 7.36 mΩ, 8.388 mΩ, 8.101 mΩ, 8.53 mΩ, and 3.53 mΩ, respectively. Notably, resistance decreases with an increase in Fe_3O_4 concentration, reaching the lowest at 70% with 3.53 mΩ.

Further examination into the electrical capacitance at the same Fe_3O_4 concentrations revealed capacitance values of 5.4×10^{-11} F, 2.8×10^{-11} F, 4.2×10^{-11} F, 2.69×10^{-10} F, and 1.6×10^{-11} F, respectively. Figure 4 illustrates an initial increase in capacitance with concentration, peaking at 60%, before a decline at 70%.

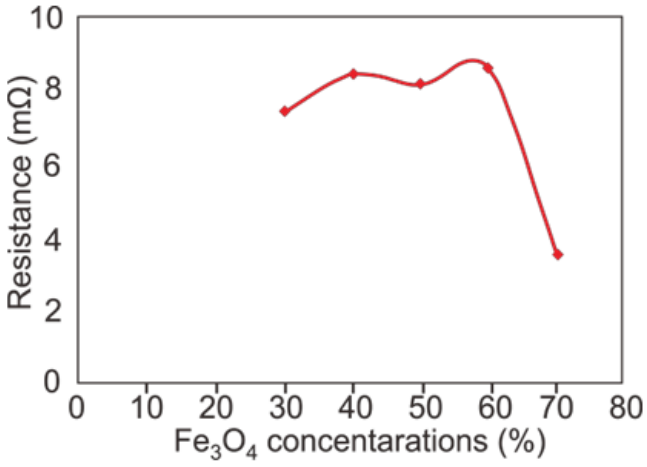

Figure 3: Graph showing the correlation between Fe_3O_4 concentration and electrical resistance in Fe_3O_4 /PANI nanocomposite layers

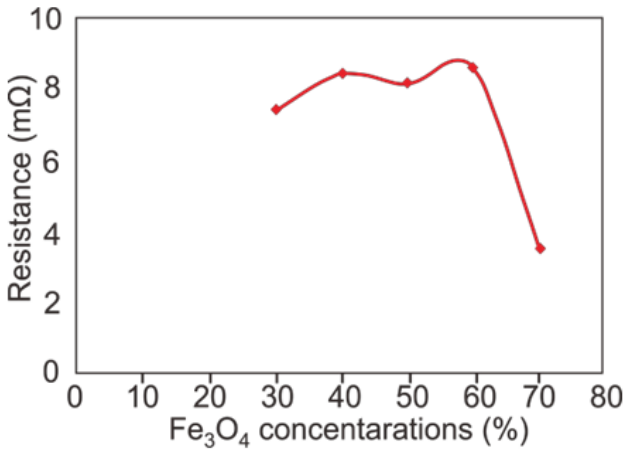

Figure 4: Graph illustrating the relationship between Fe_3O_4 concentration and electrical capacitance in Fe_3O_4 /PANI nanocomposite layers

These findings highlight the significant impact of Fe_3O_4 concentration on the electrical properties of the nanocomposites. The decrease in resistance with higher Fe_3O_4 concentration suggests improved conductivity, likely due to the greater presence of conductive Fe_3O_4 particles. Conversely, capacitance exhibits a complex relationship with concentration, peaking at 60% then decreasing, likely due to interactions between the dielectric properties of the PANI matrix and the conductive nature of Fe_3O_4 particles. These insights are pivotal for optimizing Fe_3O_4/ PANI nanocomposites' application in electronic devices [69-71].

Electrochemical response of Fe_3O_4/PANI nanocomposite

The electrochemical performance of Fe_3O_4 /PANI nanocomposite-based supercapacitor electrodes was assessed through Electrochemical Impedance Spectroscopy (EIS) using a CS350 EIS Potentiostat/Galvanostat (Corrtest Instruments, China) over a frequency range from 1 Hz to 30,000 Hz. The EIS measurements, set at an amplitude of 5 mV and a bias of 0 V DC in a 6 M KOH electrolyte using Ag/AgCl reference electrodes, are depicted in Figures 5 and 6.

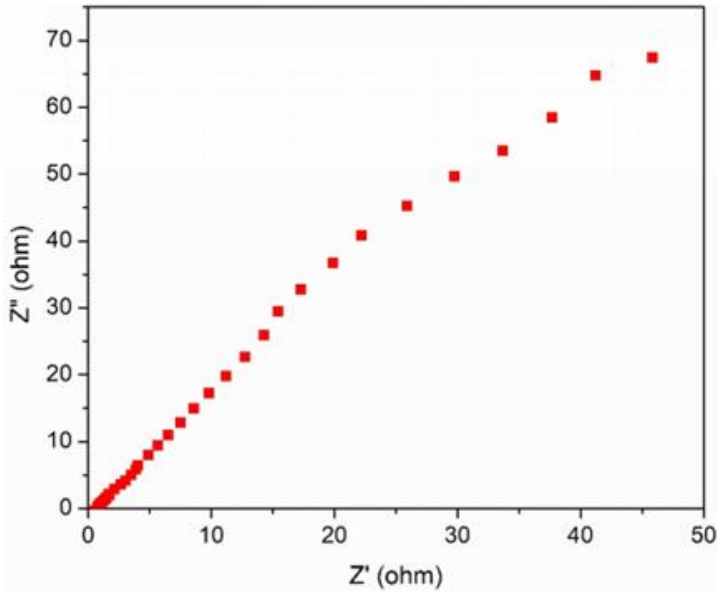

Figure 5: Nyquist plot for Fe_3O_4/PANI nanocomposite electrode with 60% Fe_3O_4 by weight

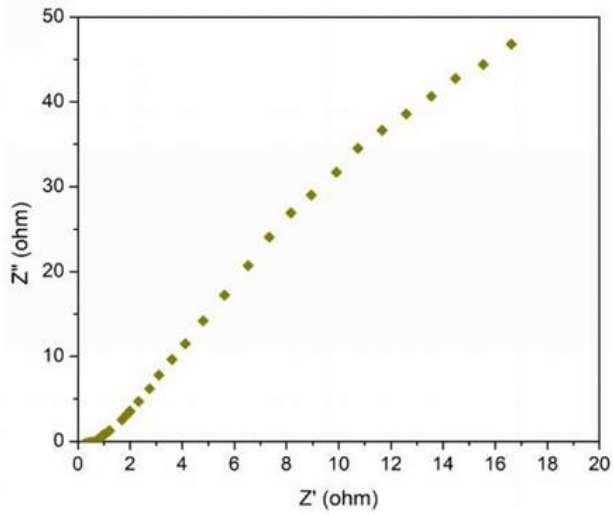

Figure 6: Nyquist plot for Fe_3O_4/PANI nanocomposite electrode with 70% Fe_3O_4 by weight

The Nyquist plots show characteristic impedance behaviours, with straight lines in both high and low frequency regions, indicating optimal electrochemical impedance characteristics. The equivalent series resistance (ESR) was approximately 0.8 Ω, reflecting the combined resistances of the Fe_3O_4 /PANI nanocomposite, the electrolyte's ionic resistance, and the contact resistance at the interface with the current collector [72].

These results illuminate the efficient electron transport within the supercapacitor, underscoring the potential of the Fe_3O_4/PANI nanocomposite for high-performance energy storage applications. The impedance behaviour across frequency regions also provides insights into charge transport mechanisms and electrode-electrolyte interactions, crucial for the design and optimization of Fe_3O_4/PANI nanocomposite-based supercapacitors [73-77].

Conclusion

The synthesis of Fe_3O_4 /PANI nanocomposites through sol-gel and spin-coating techniques marks a significant advancement in materials science. Characterization revealed distinct diffraction peaks for Fe_3O_4, PANI, and their composite, indicating successful integration. Electrophysically, these nanocomposites demonstrated a low resistance of 3.53 mΩ at a 70% Fe_3O_4 concentration and a peak capacitance of 2.69×10^{-10} F at 60% concentration. Such electrical properties highlight the potential of Fe_3O_4 /PANI nanocomposites as supercapacitor electrodes, promising for advanced energy storage applications. This research not only confirms the successful combination of Fe_3O_4 and PANI, but also establishes a foundation for further exploration and optimization of these materials in cutting-edge energy storage technologies.

Disclosure Statement

No potential conflict of interest was reported by the authors.

Funding

This work was supported by the Lembaga Penelitian dan Pengabdian Masyarakat Universitas Negeri Padang. The authors gratefully acknowledge the financial assistance for this research provided under contract number 238/UN35/LT/2022.

Authors' Contributions

All authors contributed to data analysis, drafting, and revising of the paper and agreed to be responsible for all the aspects of this work.

ORCID

Yenni Darvina
https://orcid.org/0009-0000-8971-5181
Desnita Desnita
https://orcid.org/0000-0002-7179-9871

Rahadian Zainul
https://orcid.org/0000-0002-3740-3597
Imtiaz Ali Laghari
https://orcid.org/0000-0001-5091-0297
Azril Azril
https://orcid.org/0000-0001-8685-5517
Mohammad Abdullah
https://orcid.org/0000-0003-1775-7926

References

[1]. Khan F.N.U., Rasul M.G., Sayem A., Mandal N.K., Design and optimization of lithium-ion battery as an efficient energy storage device for electric vehicles: A comprehensive review, *Journal of Energy Storage*, 2023, **71**:108033 [Crossref], [Google Scholar], [Publisher]

[2]. Patel M., Mishra K., Banerjee R., Chaudhari J., Kanchan D., Kumar D., Fundamentals, recent developments and prospects of Lithium and non-Lithium electrochemical rechargeable battery systems, *Journal of Energy Chemistry*, 2023, [Crossref], [Google Scholar], [Publisher]

[3]. Nzereogu P., Omah A., Ezema F., Iwuoha E., Nwanya A., Anode materials for lithium-ion batteries: A review, *Applied Surface Science Advances*, 2022, **9**:100233 [Crossref], [Google Scholar], [Publisher]

[4]. Hossain M.H., Chowdhury M.A., Hossain N., Islam, M.A., Mobarak M.H., Advances of lithium-ion batteries anode materials—A review, *Chemical Engineering Journal Advances*, 2023, **16**:100569 [Crossref], [Google Scholar], [Publisher]

[5]. Lavagna L., Meligrana G., Gerbaldi C., Tagliaferro A., Bartoli M., Graphene and lithium-based battery electrodes: a review of recent literature, *Energies*, 2020, **13**:4867 [Crossref], [Google Scholar], [Publisher]

[6]. Hu B., Wang X., Advances in micro lithium-ion batteries for on-chip and wearable applications, *Journal of Micromechanics and Microengineering*, 2021, **31**:114002 [Crossref], [Google Scholar], [Publisher]

[7]. Nurashikin A.A., Isa I.M., Hashim N., Ahmad M.S., Zainul R., Siti N.A.M.Y., Saidin M.I., Suyanta S., Ulianas A., Mawardi M., Synergistic Effect of Zinc/aluminium-layered Double Hydroxide-clopyralid Carbon Nanotubes Paste Electrode in the Electrochemical Response of Dopamine, Acetaminophen, and Bisphenol A, *International Journal of Electrochemical Science*, 2020, **15**:9088 [Google Scholar], [Publisher]

[8]. Zainul R., Isa I.M., Yazid A.M., Nur S., Hashim N., Mohd Sharif S.N., Saidin M.I., Ahmad M.S., Suyanta M.S., Amir Y., Enhanced electrochemical sensor for electrocatalytic glucose analysis in orange juices and milk by the integration of the electron-withdrawing substituents on graphene/glassy carbon electrode, *Journal of Analytical Methods in Chemistry*, 2022, **2022** [Crossref], [Google Scholar], [Publisher]

[9]. Abd Azis N., Isa I.M., Hashim N., Ahmad M.S., Yazid S.N.A.M., Saidin M.I., Si S.M., Zainul R., Ulianas A., Mawardi M., Synergistic effect of zinc/aluminium-layered double hydroxide-clopyralid carbon nanotubes paste electrode in the electrochemical response of dopamine, acetaminophen, and bisphenol A, *International Journal of Electrochemical Science*, 2020, **15**:9088 [Crossref], [Google Scholar], [Publisher]

[10]. Choi J.W., Aurbach D., Promise and reality of post-lithium-ion batteries with high energy densities, *Nature reviews materials*, 2016, **1**:1 [Crossref], [Google Scholar], [Publisher]

[11]. Ge Y., Jiang H., Zhu J., Lu Y., Chen C., Hu Y., Qiu Y., Zhang X., High cyclability of carbon-coated TiO2 nanoparticles as anode for sodium-ion batteries, Electrochimica Acta, 2015, **157**:142 [Crossref], [Google Scholar], [Publisher]

[12]. Liu C., Li F., Ma L.P., Cheng H.M., Advanced materials for energy storage, Advanced Materials, 2010, **22**:E28 [Crossref], [Google Scholar], [Publisher]

[13]. Zhou X., Dai Z., Liu S., Bao J., Guo Y.G., Ultra-uniform SnOx/carbon nanohybrids toward advanced lithium-ion battery anodes, Advanced Materials, 2014, **26**:3943 [Crossref], [Google Scholar], [Publisher]

[14]. Mohd Yazid S.N.A., Md Isa I., Ali N.M., Hashim N., Saidin M.I., Ahmad M.S., Asiri A.M., Khan A., Zainul R., Graphene/iridium (III) dimer complex composite modified glassy carbon electrode as selective electrochemical sensor for determination of hydroquinone in real-life water samples, International Journal of Environmental Analytical Chemistry, 2022, **102**:2607 [Crossref], [Google Scholar], [Publisher]

[15]. Rais N.S.M., Isa, I.M., Hashim N., Saidin M.I., Yazid S.N.A.M., Ahmad M.S., Zainul R., Mukdasai S., Simultaneously determination of bisphenol A and uric acid by zinc/aluminum-layered double hydroxide-2-(2, 4-dichlorophenoxy) propionate paste electrode, International Journal of Electrochemical Science, 2019, **14**:7911 [Crossref], [Google Scholar], [Publisher]
[16]. Zainul R., Hashim N., Yazid S.N.A.M., Sharif S.N.M., Ahmad M.S., Saidin M.I., Sobry M., Isa I.M., Magnesium layered hydroxide-3-(4-methoxyphenyl) propionate modified single-walled carbon nanotubes as sensor for simultaneous determination of Bisphenol A and Uric Acid, International Journal of Electrochemical Science, 2021, **16**:210941 [Crossref], [Google Scholar], [Publisher]
[17]. Abd Azis N., Isa I.M., Hashim N., Ahmad M.S., Yazid S.N.A.M., Saidin M.I., Si S.M., Zainul R., Ulianas A., Mukdasai S., Voltammetric determination of bisphenol a in the presence of uric acid using a zn/al-ldh-qm modified MWCNT paste electrode, International Journal of Electrochemical Science, 2019, **14**:10607 [Crossref], [Google Scholar], [Publisher]
[18]. Kulpa-Koterwa A., Ossowski T., Niedziałkowski P. Functionalized Fe_3O_4 nanoparticles as glassy carbon electrode modifiers for heavy metal ions detection—a mini review. *Materials*, 2021, **14**:7725 [Crossref], [Google Scholar], [Publisher]
[19]. Liu M., Ye Y., Ye J., Gao T., Wang D., Chen G., Song Z., Recent Advances of Magnetite (Fe3O4)-Based Magnetic Materials in Catalytic Applications, Magnetochemistry, 2023, **9**:110 [Crossref], [Google Scholar], [Publisher]
[20]. Velásquez C., Vásquez F., Alvarez-Láinez M., Zapata-González A., Calderón J., Carbon nanofibers impregnated with Fe3O4 nanoparticles as a flexible and high capacity negative electrode for lithium-ion batteries, *Journal of Alloys and Compounds*, 2021, **862**:158045 [Crossref], [Google Scholar], [Publisher]
[21]. Pop D., Buzatu R., Moacă E.A., Watz C.G., Cîntă Pînzaru S., Barbu Tudoran L., Nekvapil F., Avram Ş., Dehelean C.A., Creţu M.O., Development and Characterization of Fe3O4@ Carbon Nanoparticles and Their Biological Screening Related to Oral Administration, *Materials*, 2021, **14**:3556 [Crossref], [Google Scholar], [Publisher]
[22]. Nguyen M.D., Tran H.V., Xu S., Lee T.R., Fe3O4 Nanoparticles: Structures, synthesis, magnetic properties, surface functionalization, and emerging applications, *Applied Sciences*, 2021, **11**:11301 [Crossref], [Google Scholar], [Publisher]
[23]. Hasanudin H., Asri W.R., Zulaikha I.S., Ayu C., Rachmat A., Riyanti F., Hadiah F., Zainul R., Maryana R., Hydrocracking of crude palm oil to a biofuel using zirconium nitride and zirconium phosphide-modified bentonite, *RSC advances*, 2022, **12**:21916 [Crossref], [Google Scholar], [Publisher]
[24]. Tajudin M.H.A., Ahmad M.S., Isa I.M., Hashim, N., Ul-Hamid A., Saidin M.I., Zainul R., Si S.M., Sensitive determination of uric acid at layered zinc hydroxide-sodium dodecyl sulphate-propoxur nanocomposite, *Journal of Electrochemical Science and Engineering*, 2022, **12**:331 [Google Scholar], [Publisher]
[25]. Wu Z.S., Zheng Y., Zheng S., Wang S., Sun C., Parvez K., Ikeda T., Bao X., Müllen K., Feng X., Stacked-layer heterostructure films of 2D thiophene nanosheets and graphene for high-rate all-solid-state pseudocapacitors with enhanced volumetric capacitance, *Advanced Materials*, 2017, **29**:1602960 [Crossref], [Google Scholar], [Publisher]
[26]. Kurc B., Pigłowska M., Rymaniak Ł., Fuć P., Modern nanocomposites and hybrids as electrode materials used in energy carriers, *Nanomaterials*, 2021, **11**:538 [Crossref], [Google Scholar], [Publisher]
[27]. Liu Z., Zheng F., Xiong W., Li X., Yuan A., Pang H., Strategies to improve electrochemical performances of pristine metal-organic frameworks-based electrodes for lithium/sodium-ion batteries, *SmartMat*, 2021, **2**:488 [Crossref], [Google Scholar], [Publisher]
[28]. Khalafallah D., Li X., Zhi M., Hong Z., Nanostructuring nickel–zinc–boron/graphitic carbon nitride as the positive electrode and BiVO4-immobilized nitrogen-doped defective carbon as the negative electrode for asymmetric capacitors, *ACS Applied Nano Materials*, 2021, **4**:14258 [Crossref], [Google Scholar], [Publisher]

[29]. Mohanty R., Swain G., Parida K., Parida K., Enhanced electrochemical performance of flexible asymmetric supercapacitor based on novel nanostructured activated fullerene anchored zinc cobaltite, *Journal of Alloys and Compounds*, 2022, **919**:165753 [Crossref], [Google Scholar], [Publisher]
[30]. Rahmawati F., Heliani K.R., Wijayanta A.T., Zainul R., Wijaya K., Miyazaki T., Miyawaki J., Alkaline leaching-carbon from sugarcane solid waste for screen-printed carbon electrode, *Chemical Papers*, 2023, **77**:3399 [Crossref], [Google Scholar], [Publisher]
[31]. Rahmadiawan D., Abral H., Ilham M.K., Puspitasari P., Nabawi R.A., Shi S.C., Sugiarti E., Muslimin A.N., Chandra D., Ilyas R., Enhanced UV blocking, tensile and thermal properties of bendable TEMPO-oxidized bacterial cellulose powder-based films immersed in PVA/Uncaria gambir/ZnO solution, *Journal of materials research and technology*, 2023, **26**:5566 [Crossref], [Google Scholar], [Publisher]
[32]. Sharma K., Arora A., Tripathi S.K., Review of supercapacitors: Materials and devices, *Journal of Energy Storage*, 2019, **21**:801 [Crossref], [Google Scholar], [Publisher]
[33]. Dutta A., Mitra S., Basak M., Banerjee T., A comprehensive review on batteries and supercapacitors: development and challenges since their inception, *Energy Storage*, 2023, **5**:e339 [Crossref], [Google Scholar], [Publisher]
[34]. Mallick P., Moharana S., Biswal L., Satpathy S.K., Transition Metal Oxide-Based Nanomaterials for Advanced Energy Storage, *Emerging Nanodielectric Materials for Energy Storage: From Bench to Field, Springer International Publishing*, 2023, 331 [Crossref], [Google Scholar], [Publisher]
[35]. Κοιλάκος Ν.Ε., Failure diagnostics and recycling of lithium-ion batteries, *Bachelor's thesis*, 2023 [Google Scholar], [Publisher]
[36]. Putri G.E., Gusti F.R., Sary A.N., Zainul R., Synthesis of silver nanoparticles used chemical reduction method by glucose as reducing agent, *Journal of Physics: Conference Series*, 2019, **1317**:012027 [Crossref], [Google Scholar], [Publisher]
[37]. Zainul R., Oktavia B., Dewat I., Efendi J., Study of Internal Morphology on Preparation of Cu2OThin-Plate using Thermal Oxidation, *Journal of Physics: Conference Series*, 2018, **1116**: 042046 [Crossref], [Google Scholar], [Publisher]
[38]. Mohd Sharif S.N., Hashim N., Md Isa I., Abu Bakar S., Idris Saidin M., Syahrizal Ahmad M., Mamat M., Zobir Hussein M., Zainul R., Carboxymethyl cellulose hydrogel based formulations of zinc hydroxide nitrate-sodium dodecylsulphate-bispyribac nanocomposite: Advancements in controlled release formulation of herbicide, *Journal of nanoscience and nanotechnology*, 2021, **21**:5867 [Crossref], [Google Scholar], [Publisher]
[39]. Zhao J., Burke A.F., Electrochemical capacitors: Materials, technologies and performance, *Energy Storage Materials*, 2021, **36**:31 [Crossref], [Google Scholar], [Publisher]
[40]. Lamb J.J., Burheim O.S., Lithium-ion capacitors: A review of design and active materials, *Energies*, 2021, **14**:979 [Crossref], [Google Scholar], [Publisher]
[41]. Liu Y., Yu Z., Chen J., Li C., Zhang Z., Yan X., Liu X., Yang S., Recent development and progress of structural energy devices, *Chinese Chemical Letters*, 2022, **33**:1817 [Crossref], [Google Scholar], [Publisher]
[42]. Sharif S.N., Hashim N., Isa I.M., Bakar S.A., Saidin M.I., Ahmad M.S., Mamat M., Hussein M.Z., Zainul R., Chitosan as a coating material in enhancing the controlled release behaviour of zinc hydroxide nitrate–sodium dodecylsulphate–bispyribac nanocomposite, *Chemical Papers*, 2021, **75**:611 [Crossref], [Google Scholar], [Publisher]
[43]. Rahmadiawan D., Abral H., Shi S.C., Huang T.T., Zainul R., Nurdin H., Tribological Properties of Polyvinyl Alcohol/Uncaria Gambir Extract Composite as Potential Green Protective Film, *Tribology in Industry*, 2023, **45** [Crossref], [Google Scholar], [Publisher]
[44]. Fu W., Turcheniuk K., Naumov O., Mysyk R., Wang F., Liu M., Kim D., Ren X., Magasinski A., Yu M., Materials and technologies for multifunctional, flexible or integrated supercapacitors and batteries, *Materials Today*, 2021, **48**:176 [Crossref], [Google Scholar], [Publisher]
[45]. Rani S., Kumar N., Sharma Y., Recent progress and future perspectives for the

development of micro-supercapacitors for portable/wearable electronics applications, *Journal of Physics: Energy*, 2021, **3**:032017 [Crossref], [Google Scholar], [Publisher]
[46]. Swain N., Tripathy A., Thirumurugan A., Saravanakumar B., Schmidt-Mende L., Ramadoss A., A brief review on stretchable, compressible, and deformable supercapacitor for smart devices, *Chemical Engineering Journal*, 2022, **446**:136876 [Crossref], [Google Scholar], [Publisher]
[47]. Zhou Y., Qi H., Yang J., Bo Z., Huang F., Islam M.S., Lu X., Dai L., Amal R., Wang C.H., Two-birds-one-stone: multifunctional supercapacitors beyond traditional energy storage, *Energy & Environmental Science*, 2021, **14**:1854 [Crossref], [Google Scholar], [Publisher]
[48]. Lee J.H., Yang G., Kim C.H., Mahajan R.L., Lee S.Y., Park S.J., Flexible solid-state hybrid supercapacitors for the internet of everything (IoE), *Energy & Environmental Science*, 2022, **15**:2233 [Crossref], [Google Scholar], [Publisher]
[49]. Das H.T., Dutta S., Balaji T.E., Das N., Das P., Dheer N., Kanojia R., Ahuja P., Ujjain S.K., Recent trends in carbon nanotube electrodes for flexible supercapacitors: a review of smart energy storage device assembly and performance, *Chemosensors*, 2022, **10**:223 [Crossref], [Google Scholar], [Publisher]
[50]. Hsu H.H., Multifunctional flexible conductive materials for supercapacitors and biosensors, 2021 [Google Scholar], [Publisher]
[51]. Jia R., Shen G., Qu F., Chen D., Flexible on-chip micro-supercapacitors: Efficient power units for wearable electronics, *Energy Storage Materials*, 2020, **27**:169 [Crossref], [Google Scholar], [Publisher]
[52]. Wang G., Zhang L., Zhang J., A review of electrode materials for electrochemical supercapacitors, *Chemical Society Reviews*, 2012, **41**:797 [Crossref], [Google Scholar], [Publisher]
[53]. Iro Z.S., Subramani C., Dash S., A brief review on electrode materials for supercapacitor, *International Journal of Electrochemical Science*, 2016, **11**:10628 [Crossref], [Google Scholar], [Publisher]
[54]. Zheng S., Wu Z.S., Wang S., Xiao H., Zhou F., Sun C., Bao X., Cheng H.M., Graphene-based materials for high-voltage and high-energy asymmetric supercapacitors, *Energy Storage Materials*, 2017, **6**:70 [Crossref], [Google Scholar], [Publisher]
[55]. Shaikh N.S., Ubale S.B., Mane V.J., Shaikh J.S., Lokhande V.C., Praserthdam S., Lokhande C.D., Kanjanaboos P., Novel electrodes for supercapacitor: Conducting polymers, metal oxides, chalcogenides, carbides, nitrides, MXenes, and their composites with graphene, *Journal of Alloys and Compounds*, 2022, **893**:161998 [Crossref], [Google Scholar], [Publisher]
[56]. Abdah M.A.A.M., Azman N.H.N., Kulandaivalu S., Sulaiman Y., Review of the use of transition-metal-oxide and conducting polymer-based fibres for high-performance supercapacitors, *Materials & Design*, 2020, **186**:108199 [Crossref], [Google Scholar], [Publisher]
[57]. Reddy P.H., Amalraj J., Ranganatha S., Patil S.S., Chandrasekaran S., A review on effect of conducting polymers on carbon-based electrode materials for electrochemical supercapacitors, *Synthetic Metals*, 2023, **298**:117447 [Crossref], [Google Scholar], [Publisher]
[58]. Yasami S., Mazinani S., Abdouss M., Developed composites materials for flexible supercapacitors electrode:"Recent progress & future aspects", *Journal of Energy Storage*, 2023, **72**:108807 [Crossref], [Google Scholar], [Publisher]
[59]. Dhandapani E., Thangarasu S., Ramesh S., Ramesh K., Vasudevan R., Duraisamy N., Recent development and prospective of carbonaceous material, conducting polymer and their composite electrode materials for supercapacitor—A review, *Journal of Energy Storage*, 2022, **52**:104937 [Crossref], [Google Scholar], [Publisher]
[60]. Veerakumar P., Sangili A., Manavalan S., Thanasekaran P., Lin K.C., Research progress on porous carbon supported metal/metal oxide nanomaterials for supercapacitor electrode applications, *Industrial & engineering chemistry research*, 2020, **59**:6347 [Crossref], [Google Scholar], [Publisher]
[61]. Darvina Y., Rianto D., Murti F., Yulfriska N., Ramli. Struktur Nano Partikel Besi Oksida dari Pasir Besi Pantai Tiram Sumatera Barat. Prosiding Semirata BKS Bidang MIPA Wilayah Barat, Universitas Jambi, 2017. [Publisher]

[62]. Darvina Y., Yulfriska N., Rifai H., Dwiridal L., Ramli R., Synthesis of magnetite nanoparticles from iron sand by ball-milling, *Journal of Physics: Conference Series*, 2019, **1185**:012017 [Crossref], [Google Scholar], [Publisher]
[63]. Londoño-Restrepo S.M., Jeronimo-Cruz, R., Millán-Malo, B.M., Rivera-Muñoz, E.M.,Rodriguez-García, M.E., Effect of the nano crystal size on the X-ray diffraction patterns of biogenic hydroxyapatite from human, bovine, and porcine bones, *Scientific Reports*, 2019, **9**:5915 [Crossref], [Google Scholar], [Publisher]
[64]. Hassanzadeh-Tabrizi S.A., Precise calculation of crystallite size of nanomaterials: a review, *Journal of Alloys and Compounds*, 171914 [Crossref], [Google Scholar], [Publisher]
[65]. Al-Harbi N., Enhancement of the optical and electrical properties of poly ethyl methacrylate/polyvinyl chloride-zinc sulphide (PEMA/PVC@ ZnS) ternary nanocomposite films, *Heliyon*, 2023, **9** [Crossref], [Google Scholar], [Publisher]
[66]. Zhu J., Zhou S., Li M., Xue A., Zhao Y., Peng W., Xing W., PVDF mixed matrix ultrafiltration membrane incorporated with deformed rebar-like Fe3O4–palygorskite nanocomposites to enhance strength and antifouling properties, *Journal of Membrane Science*, 2020, **612**:118467 [Crossref], [Google Scholar], [Publisher]
[67]. Veeman D., Shree M.V., Sureshkumar P., Jagadeesha T., Natrayan L., Ravichandran M., Paramasivam P., Sustainable development of carbon nanocomposites: synthesis and classification for environmental remediation, *Journal of Nanomaterials*, 2021, **2021**:1 [Crossref], [Google Scholar], [Publisher]
[68]. Bandehali S., Parvizian F., Ruan H., Moghadassi A., Shen J., Figoli A., Adeleye A.S., Hilal N., Matsuura T., Drioli E., A planned review on designing of high-performance nanocomposite nanofiltration membranes for pollutants removal from water, *Journal of Industrial and Engineering Chemistry*, 2021, **101**:78 [Crossref], [Google Scholar], [Publisher]
[69]. Li Z., Gong L., Research progress on applications of polyaniline (PANI) for electrochemical energy storage and conversion, *Materials*, 2020, **13**:548 [Crossref], [Google Scholar], [Publisher]
[70]. Pina C.D., Falletta E., Advances in polyaniline for biomedical applications, *Current medicinal chemistry*, 2022, **29**:329 [Crossref], [Google Scholar], [Publisher]
[71]. Mathai S., Shaji P., Polymer-Based Nanocomposite Coating Methods: A Review, *Journal of Scientific Research*, 2022, **14**:973 [Crossref], [Google Scholar], [Publisher]
[72]. Ma Y., Hou C., Zhang H., Zhang Q., Liu H., Wu S., Guo Z., Three-dimensional core-shell Fe3O4/Polyaniline coaxial heterogeneous nanonets: Preparation and high performance supercapacitor electrodes, *Electrochimica Acta*, 2019, **315**:114 [Crossref], [Google Scholar], [Publisher]
[73]. Badawy I.M., Elbanna A.M., Ramadan M., Allam N.K., Propping the electrochemical impedance spectra at different voltages reveals the untapped supercapacitive performance of materials, *Electrochimica Acta*, 2022, **408**:139932 [Crossref], [Google Scholar], [Publisher]
[74]. Zeng Y., Hu J., Yang J., Tang P., Fu Q., Zhou W., Peng Y., Xiao P., Chen S., Guo K., Mechanistic insights into the pseudocapacitive performance of bronze-type vanadium dioxide with mono/multi-valent cations intercalation, *Journal of Materials Chemistry A*, 2022, **10**:10439 [Crossref], [Google Scholar], [Publisher]
[75]. Schutjajew K., Tichter T., Schneider J., Antonietti M., Roth C., Oschatz M., Insights into the sodiation mechanism of hard carbon-like materials from electrochemical impedance spectroscopy, *Physical Chemistry Chemical Physics*, 2021, **23**:11488 [Crossref], [Google Scholar], [Publisher]
[76]. Sadegh F., Modarresi-Alam A.R., Sadegh N., Bahrpeyma A., Shabzendedar S., Kerman K., Noroozifar M. Simple and green route for fabrication of a nanostructured graphene-Fe_3O_4@ PANI for the photovoltaic activity. *Electrochimica Acta*, 2021, **399**:139327 [Crossref], [Google Scholar], [Publisher]
[77]. Sadegh F., Modarresi-Alam A.R., Sadegh N., Bahrpeyma A., Shabzendedar S., Kerman K., Noroozifar M., Simple and green route for fabrication of a nanostructured of the graphene-Fe3O4@ PANI for the photovoltaic activity, *Electrochimica Acta*, 2021, **399**:139327 [Crossref], [Google Scholar], [Publisher]

HOW TO CITE THIS ARTICLE
Yenni Darvina, Desnita Desnita*, Rahadian Zainul, Imtiaz Ali Laghari, Azril Azril, Mohammad Abdullah, Advancements in Fe_3O_4/PANI Nanocomposite Film Technology: Synthesis and Characterization. *J. Med. Chem. Sci*., 2024, 7(5) 689-702.
DOI: https://doi.org/10.26655/JMCHEMSCI.2024.5.5
URL: https://www.jmchemsci.com/article_190828.html